Inhomogeneous chiral condensates within the Functional Renormalization Group (FRG)

Part of CRC-TR 211 Project A03: Inhomogeneous phases at high density

M. J. Steil[1], M. Buballa[1] and B.-J. Schaefer[2]

[1]Technische Universität Darmstadt
[2]Justus-Liebig-Universität Gießen

Lunch Club Seminar, Gießen, July 11, 2018

Outline

Motivation: QCD phase diagram at low T

- Standard argument for a QCD critical point:
  - Lattice: crossover at high T and low μ
  - Models: 1st order at low T and high μ

$\Rightarrow$ based on tacit assumption: $\langle\bar{q}q\rangle(\vec{x})$ constant in space/ homogeneous

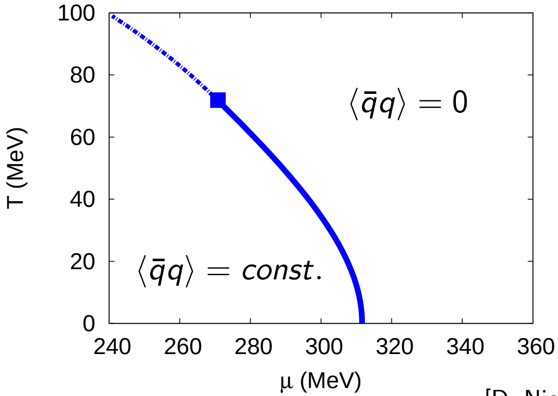

[D. Nickel, PRD (2009)]

Motivation: QCD phase diagram at low T

- Allowing for $\langle \bar{q}q \rangle (\vec{x}) \Rightarrow$ energetically favored inhomogeneous condensates overlapping the 1st order transition
  - Critical point $\rightarrow$ Lifshitz point [D. Nickel, PRD (2009)]
  - Inhomogeneous phase rather robust under model extensions and variations [M. Buballa, S. Carignano, PPNP (2015)]

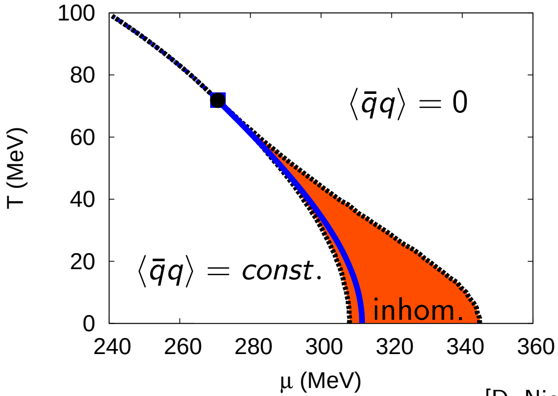

[D. Nickel, PRD (2009)]

- **Motivation:** Open questions regarding the stability of inhomogeneous chiral condensates under quantum and thermal fluctuations
- **Current goal:** Study effects of bosonic and fermionic quantum fluctuations on inhomogeneous chiral condensates in the Quark-Meson (QM) model
  - $N_f = 2$ QM model in the chiral limit as effective, low-energy model of QCD
  - Chiral density wave (CDW) ansatz for the chiral condensate
- **Method:** Study within the *Functional Renormalization Group* (FRG)
  - Highly potent tool to investigate effects of quantum fluctuations
  - In-medium computations ($T \geq 0$ and $\mu \geq 0$) are possible without fundamental problems
  - Inclusion of inhomogeneous condensates is formally unproblematic

- Exact implementation of Wilson's RG approach:

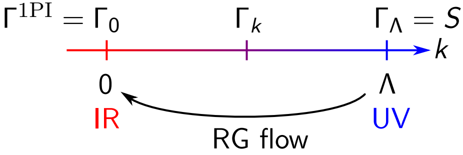

- [C. Wetterich, PLB (1993)]: **exact RG/ Wetterich/ flow equation**:

$$\partial_k \Gamma_k = -\mathrm{Tr}\left[\left(\frac{\overrightarrow{\delta}}{\delta\bar{\psi}}\Gamma_k\frac{\overleftarrow{\delta}}{\delta\psi} + R_k^F\right)^{-1}\partial_k R_k^F\right] + \frac{1}{2}\mathrm{Tr}\left[\left(\frac{\delta}{\delta\phi}\frac{\delta}{\delta\phi}\Gamma_k + R_k^B\right)^{-1}\partial_k R_k^B\right]$$

$=$ $-$ 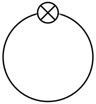 $+\frac{1}{2}$ 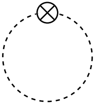

Two flavor Quark-Meson model in LPA

- Truncation of Γ_k is necessary to explicitly solve the flow equation
  - Lowest-order *derivative expansion*: **Local potential approximation (LPA) for QM model**:

$$\Gamma_{k}[\psi,\bar{\psi},\phi] = \int \mathrm{d}^4 z \Big\{ \bar{\psi}(z) \left[\partial\!\!\!/ - \mu\gamma_0 + g\left(\sigma(z) + \mathrm{i}\gamma_5 \vec{\tau}\cdot\vec{\pi}(z)\right)\right] \psi(z) + \frac{1}{2}\left(\partial_\mu \phi(z)\right)\left(\partial^\mu \phi(z)\right) + U_{k}(\phi(z)\phi(z)) \Big\}$$

- **Chiral density wave (CDW) ansatz for the expectation values/ condensates:**

$$\phi(z) \overset{CDW}{=} \left(\sigma(\vec{z}), 0, 0, \pi(\vec{z})\right) = \frac{M}{g}\left(\cos(\vec{q}\cdot\vec{z}), 0, 0, \sin(\vec{q}\cdot\vec{z})\right)$$

$$\rho \equiv \phi(z)\phi(z) \overset{CDW}{=} \frac{M^2}{g^2} \equiv \rho$$ Spatially independent $O(4)$-sym. field

$$\phi_0(z) \pm \mathrm{i}\, O\phi_3(z) \overset{CDW}{=} \frac{M}{g} \exp\left(\pm \mathrm{i}\, O\vec{q}\cdot\vec{z}\right), \quad \text{for } O^2 = \mathbb{1}$$ *Euler's formula*

$$\Gamma_k^{(0,1,1)}(x,y) \equiv \frac{\overrightarrow{\delta}}{\delta\bar{\psi}(x)}\Gamma_k[\psi,\bar{\psi},\phi]\frac{\overleftarrow{\delta}}{\delta\psi(y)}$$

$$\overset{CDW}{=} \delta^{(4)}(x-y)\Big[\gamma_0\partial_0 - \mu\gamma_0 + \vec{\partial\!\!\!/} + M\big(\cos(\vec{q}\cdot\vec{x}) + \mathrm{i}\gamma_5\tau_3\sin(\vec{q}\cdot\vec{x})\big)\Big]$$

$$= \delta^{(4)}(x-y)\Big[\gamma_0\partial_0 - \mu\gamma_0 + \vec{\partial\!\!\!/} + M\exp\left(\mathrm{i}\gamma_5\tau_3\vec{q}\cdot\vec{x}\right)\Big]$$

$$\Gamma_k^{(2,0,0)}(x,y) \equiv \frac{\delta}{\delta\phi_i(x)}\frac{\delta}{\delta\phi_j(y)}\Gamma_k[\psi,\bar{\psi},\phi]$$

$$\overset{CDW}{=} \delta^{(4)}(x-y)\Big[\left(-\partial_x^2 + 2U_k'(\rho)\right)\delta_{ij} + 4U_k''(\rho)\phi_i(x)\phi_j(x)\Big]$$

$$\phi_i(x)\phi_j(x) \overset{CDW}{=} \rho\begin{pmatrix} \cos^2(\vec{q}\cdot\vec{x}) & 0 & 0 & \cos(\vec{q}\cdot\vec{x})\sin(\vec{q}\cdot\vec{x}) \\ 0 & 0 & 0 & 0 \\ 0 & 0 & 0 & 0 \\ \cos(\vec{q}\cdot\vec{x})\sin(\vec{q}\cdot\vec{x}) & 0 & 0 & \sin^2(\vec{q}\cdot\vec{x}) \end{pmatrix}$$

Strategy: Diagonalization using unitary operators

- It is possible to insert unitary operators ($O^\dagger O = \mathbb{1}$ and $\partial_k O = 0$) into the LPA loops:

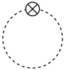

$$= \mathrm{Tr}\left[\left(\partial_k R_k^B\right)\left(\Gamma_k^{(2,0,0)} + R_k^B\right)^{-1}\right]$$

$$= \mathrm{Tr}\left[\left(\partial_k V^\dagger R_k^B V\right)\left(V^\dagger \Gamma_k^{(2,0,0)} V + V^\dagger R_k^B V\right)^{-1}\right]$$

$$= \mathrm{Tr}\left[\left(\partial_k R_{V,k}^B\right)\left(\Gamma_{k,V}^{(2,0,0)} + R_{V,k}^B\right)^{-1}\right]$$

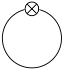

$$= \mathrm{Tr}\left[\left(\partial_k R_k^F\right)\left(\Gamma_k^{(0,1,1)} + R_k^F\right)^{-1}\right]$$

$$= \mathrm{Tr}\left[\left(\partial_k U^\dagger \gamma_0 R_k^F U\right)\left(U^\dagger \gamma_0 \Gamma_k^{(0,1,1)} U + U^\dagger \gamma_0 R_k^F U\right)^{-1}\right]$$

$$= \mathrm{Tr}\left[\left(\partial_k \tilde{R}_{U,k}^F\right)\left(\tilde{\Gamma}_{k,U}^{(0,1,1)} + \tilde{R}_{U,k}^F\right)^{-1}\right]$$

CRC-TR 211

- **For the fermionic correlator/loop:**
  - For the CDW

$$U(\vec{x}) \equiv \exp\left(-\frac{\mathrm{i}}{2}\gamma_5\tau_3\vec{q}\cdot\vec{x}\right)$$

diagonalizes $\Gamma_k^{(0,1,1)}$ in momentum space:

$$\tilde{\Gamma}_{k,U}^{(0,1,1)} \equiv U^\dagger\gamma_0\Gamma_k^{(0,1,1)}U = \delta^{(4)}(x-y)\left[\partial_0 - \mu + \gamma_0\gamma_i\partial^i - \frac{\mathrm{i}}{2}\gamma_0\gamma_i\gamma_5\tau_3 q^i + \gamma_0 M\mathbb{1}\right].$$

  - Generic (3D) fermionic regulators stay diagonal under the unitary transformation U:

$$\tilde{R}_{U,k}^F(p,r) \equiv \int\frac{\mathrm{d}^4a}{(2\pi)^4}\int\frac{\mathrm{d}^4b}{(2\pi)^4}U^\dagger(p,a)\gamma_0R_k^F(a,b)U(b,r)$$

$$= \mathrm{i}(2\pi)^4\delta^{(4)}(p-r)\left[\frac{1}{2}\left(\mathbb{1}+\gamma_5\tau_3\right)\gamma_0\left(\vec{p\!\!/}+\vec{q\!\!/}/2\right)r_k^F\left(|\vec{p}+\vec{q}/2|/k\right)\right.$$

$$\left.+\frac{1}{2}\left(\mathbb{1}-\gamma_5\tau_3\right)\gamma_0\left(\vec{p\!\!/}-\vec{q\!\!/}/2\right)r_k^F\left(|\vec{p}-\vec{q}/2|/k\right)\right].$$

- **For the bosonic correlator/loop:**
  - A change of basis Λ from $(\phi_0, \phi_3) \to (\phi_0 + \mathrm{i}\phi_3, \phi_0 - \mathrm{i}\phi_3)$ simplifies $\phi_i(x)\phi_j(x)$ dramatically:

$$\Lambda^\dagger_{in}\phi_n(x)\phi_m(x)\Lambda_{mj} = \frac{\rho}{2}\begin{pmatrix} 1 & 0 & 0 & \exp(-2\mathrm{i}\vec{q}\cdot\vec{x}) \\ 0 & 0 & 0 & 0 \\ 0 & 0 & 0 & 0 \\ \exp(2\mathrm{i}\vec{q}\cdot\vec{x}) & 0 & 0 & 1 \end{pmatrix}.$$

  - The remaining position dependence can be eliminated easily with an appropriate unitary operator $Q(\vec{x})$. The composite unitary operator

$$V(\vec{x}) \equiv \Lambda Q(\vec{x}) = \frac{1}{2}\begin{pmatrix} 1-\exp(-2\mathrm{i}\vec{q}\cdot\vec{x}) & 0 & 0 & 1+\exp(-2\mathrm{i}\vec{q}\cdot\vec{x}) \\ 0 & 2 & 0 & 0 \\ 0 & 0 & 2 & 0 \\ -\mathrm{i}(1+\exp(-2\mathrm{i}\vec{q}\cdot\vec{x})) & 0 & 0 & \mathrm{i}(\exp(-2\mathrm{i}\vec{q}\cdot\vec{x})-1) \end{pmatrix}.$$

    diagonalizes $\Gamma_k^{(2,0,0)}$ in momentum space.
  - Generic (3D) bosonic regulators stay diagonal under unitary transformation V.

Solution: LPA Flow equation

CRC-TR 211

LPA flow equation for $U_k(\rho)$ with CDW condensates

$$\partial_k U_k(\rho) = \int \frac{d^3 p}{(2\pi)^3} \sum_{i=0}^{3} \frac{1}{2} \coth\left(\frac{E_k^i}{2T}\right) \partial_k E_k^i$$
$$- N_c N_f \int \frac{d^3 p}{(2\pi)^3} \sum_{\pm} \tanh\left(\frac{E_k^\pm + \mu}{2T}\right) \partial_k E_k^\pm + \tanh\left(\frac{E_k^\pm - \mu}{2T}\right) \partial_k E_k^\pm$$

- Using generic but **three-dimensional** FRG regulators

$$R_k^F(p,r) \equiv \mathrm{i}\vec{\not p}\, r_k^F(|\vec{p}|/k)(2\pi)^4 \delta^{(4)}(p-r)$$
$$R_k^B(p,r) \equiv \vec{p}^{\,2} r_k^B(|\vec{p}|/k)(2\pi)^4 \delta^{(4)}(p-r)$$

in a unified regulator scheme

$$\left(1 + r_k^F(|\vec{p}|/k)\right)^2 = 1 + r_k^B(|\vec{p}|/k) \equiv \lambda_k(|\vec{p}|/k)^2.$$

Flowing energy eigenvalues of the CDW

- **Fermionic eigenvalues**:

$$\left(E_k^{\pm}\right)^2 = M^2 + \frac{\left(\vec{p}_k^{\,+q}\right)^2}{2} + \frac{\left(\vec{p}_k^{\,-q}\right)^2}{2} \pm \sqrt{M^2\left(\vec{p}_k^{\,+q} - \vec{p}_k^{\,-q}\right)^2 + \frac{1}{4}\left(\left(\vec{p}_k^{\,+q}\right)^2 - \left(\vec{p}_k^{\,-q}\right)^2\right)^2}$$

$$\overset{q=0}{=} M^2 + (\vec{p}_k)^2$$

with $\vec{p}_k^{\,q} \equiv \left(\vec{p} + \vec{q}/2\right)\left(1 + r_k^F\left(|\vec{p} + \vec{q}/2|/k\right)\right) = (\vec{p} + \vec{q}/2)\sqrt{\lambda_k\left(|\vec{p} + \vec{q}/2|/k\right)}$

- **Bosonic eigenvalues**:

$$\left(E_k^{1,2}\right)^2 = (\vec{p}_k)^2 + 2U_k'(\rho) \overset{q=0}{=} (\vec{p}_k)^2 + 2U_k'(\rho)$$

$$\left(E_k^{0,3}\right)^2 = \frac{1}{2}\left(\vec{p}_k\right)^2 + \frac{1}{2}\left(\vec{p}_k^{\,+4q}\right)^2 + 2U_k'(\rho) + 2\rho U_k''(\rho) \pm \sqrt{4\rho^2 U_k''(\rho)^2 + \frac{1}{4}\left(\left(\vec{p}_k^{\,+4q}\right)^2 - \left(\vec{p}_k\right)^2\right)^2}$$

$$\overset{q=0}{=} (\vec{p}_k)^2 + 2U_k'(\rho) + 4\rho U_k''(\rho)\delta_{i0}$$

Mean field approximations

- **Extended mean-field approximation (eMFA):**

$\partial_k \Gamma_k = -$ 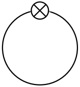 $+ \frac{1}{2}$ 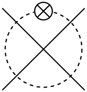

  - Neglect bosonic fluctuations and integrate the LPA flow equation

eMFA thermodynamic potential

$\bar{\Omega}^{\mathrm{eMFA}}_{\mu,T}(\sqrt{\rho}, q) \equiv \frac{\Gamma_0}{V_4} = U_\Lambda(\rho) + \frac{q^2\rho}{2} - \frac{1}{V_4}\int_\Lambda^0 \mathrm{d}k$ 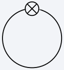

$$= \lambda_\Lambda(\rho - v_\Lambda^2)^2 + \frac{q^2\rho}{2} - N_c N_f \int \frac{\mathrm{d}^3 p}{(2\pi)^3} \sum_{\pm,\pm} T \log\left[2\cosh\left[\frac{E_k^{\pm} \pm \mu}{2T}\right]\right]_{k=\Lambda}^{k=0}$$

Mean field approximations

CRC-TR 211

- **Standard mean-field approximation (sMFA):**
  - Neglect bosonic fluctuations
  - No RG flow ($R_k^F = 1$) and evaluation of Ω at $k = 0$
  - Neglect now divergent vacuum contribution to the potential completely (*"no-sea"* approximation)
  - Test case for our numerics

sMFA thermodynamic potential

$$\bar{\Omega}^{\mathrm{sMFA}}_{\mu,T}(\sqrt{\rho}, q) \equiv \lambda_\Lambda(\rho - v_\Lambda^2)^2 + \frac{q^2\rho}{2} - N_c N_f \int \frac{\mathrm{d}^3 p}{(2\pi)^3} \cancel{\sum_{\pm} E_{k=0}^{\pm}} + T \sum_{\pm,\pm} \log\left[1 + \mathrm{e}^{-\frac{E_{k=0}^{\pm} \pm \mu}{T}}\right]$$

CRC-TR 211

Which steps are necessary to arrive at a s(/e)MFA phase-diagram?

1. Model parameter fixing in vacuum
2. Computation of the fermionic loop at different μ, T, ρ and q
   - Two dimensional momentum integrals using [*Cubature*, `https://github.com/stevengj/cubature`]
3. Minimization of $\bar{\Omega}_{\mu,T}(\sqrt{\rho}, q)$ to find $\Omega(\mu, T) = \bar{\Omega}_{\mu,T}(\sqrt{\rho}_{\mathrm{min}}, q_{\mathrm{min}})$
   - Using a spectral decomposition in Chebyshev polynomials $\mathrm{T}_{2n}(x)$

$$\bar{\Omega}_{\mu,T}(\sqrt{\rho}, q) = \sum_{n_1 n_2} a^{\mu,T}_{n_1 n_2} \mathrm{T}_{2n_1}(\sqrt{\rho}) \mathrm{T}_{2n_2}(q)$$

4. Sampling of the μ-T-plane
   - Parallelized *Block-Structured Adaptive* ~~*Mesh Refinement*~~ Sampling

Parameter fixing in the homogeneous vacuum

- Three free model parameters: Yukawa coupling g and two meson potential UV inital conditions λ_Λ and v_Λ^2
- To fix those we fit the quark mass M, the bare pion decay constant f_π and the sigma curvature mass m_σ to physical values.

$$g = \frac{M}{f_\pi}$$

$$\lambda_\Lambda = \frac{m_\sigma^2}{2f_\pi^2} + 2I''_{0,\Lambda}(f_\pi^2)$$

$$v_\Lambda^2 = f_\pi^2 \frac{m_\sigma^2 - 4I'_{0,\Lambda}(f_\pi^2) + 4f_\pi^2 I''_{0,\Lambda}(f_\pi^2)}{m_\sigma^2 + 4f_\pi^2 I''_{0,\Lambda}(f_\pi^2)}$$

with the eMFA homogeneous vacuum contribution:

$$I_{0,\Lambda}(\rho) \equiv \frac{1}{V_4}\int_\Lambda^0 \mathrm{d}k$$ 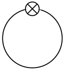 $$\Big|_{\mu=T=q=0}$$

$$= \frac{N_c N_f}{\pi^2}\int_0^\infty p^2\,\mathrm{d}p\left(\sqrt{g^2\rho + p^2\lambda_0(p)} - \sqrt{g^2\rho + p^2\lambda_\Lambda(p)}\right)$$

Parameter fixing in the homogeneous vacuum

- $f_\pi = 88\,\mathrm{MeV},\ M = 300\,\mathrm{MeV} \Rightarrow g(\Lambda) \cong 3.409 = \mathrm{const.}$
- **Exponential regulator**: $\lambda_k^{\mathrm{exp}}(y) = 1 + 1/\left(\exp(y^2) - 1\right)$

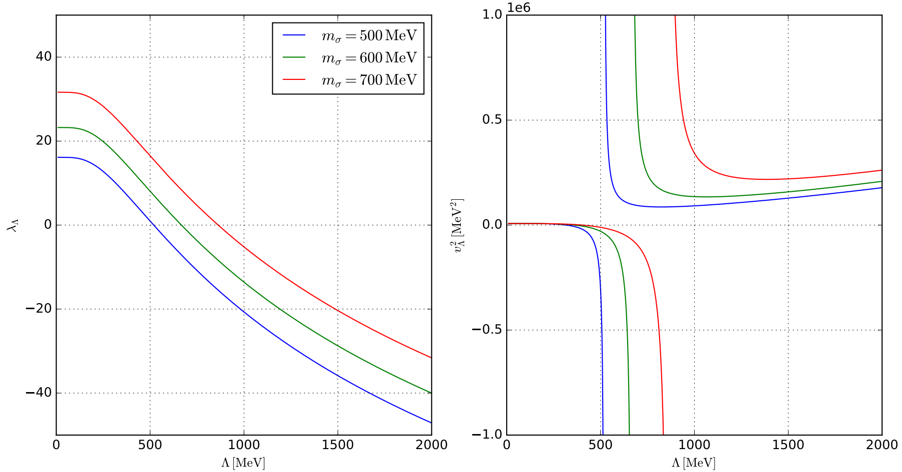

Homogeneous sMFA phase diagrams

CRC-TR 211

- $f_\pi = 88\,\mathrm{MeV}$ and $M = 300\,\mathrm{MeV}$
- $P(\sqrt{\rho} = 0) = P_\mathrm{B} + P_\mathrm{SB} = -\frac{1}{8} f_\pi^2 m_\sigma^2 + \frac{7\pi^2}{30} T^4 + T^2\mu^2 + \frac{\mu^4}{2\pi^2}$
- $\mu_\mathrm{PT}(T = 0) = \sqrt{\pi f_\pi \frac{m_\sigma}{2}}$

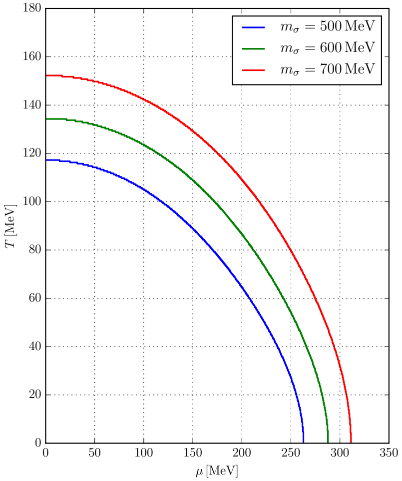

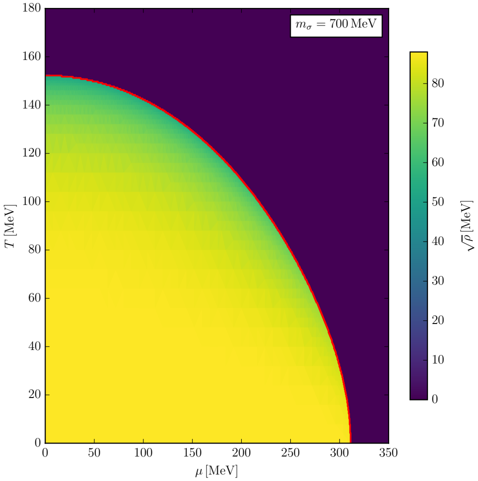

Inhomogeneous sMFA phase diagrams

- $f_\pi = 88\,\mathrm{MeV}$, $M = 300\,\mathrm{MeV}$ and $m_\sigma = 700\,\mathrm{MeV}$

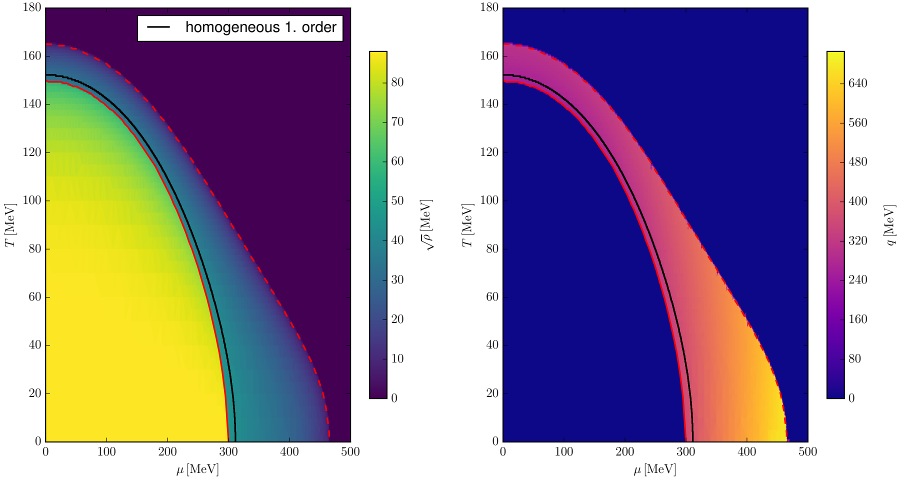

What is the "right" RG UV initial scale Λ?

- $f_\pi = 88\,\mathrm{MeV}$, $M = 300\,\mathrm{MeV}$ and $m_\sigma = 600\,\mathrm{MeV}$

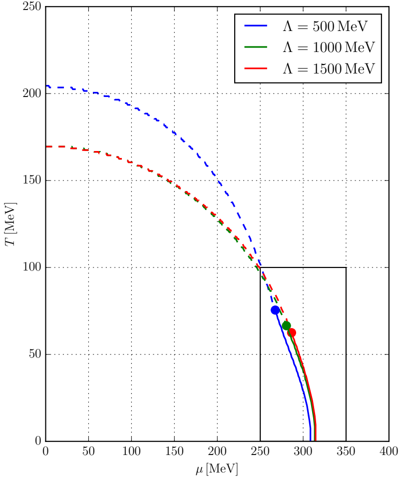

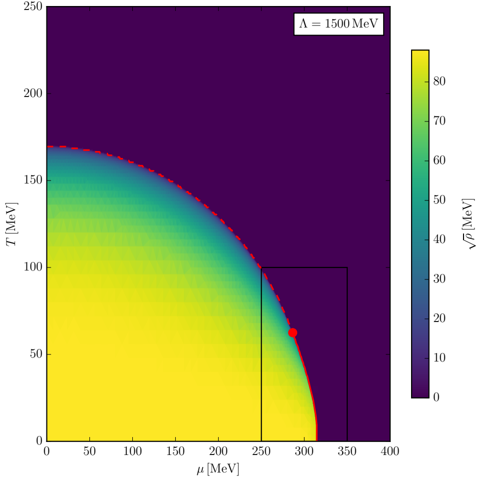

Inhomogeneous eMFA phase diagrams

- $f_\pi = 88\,\mathrm{MeV}$, $M = 300\,\mathrm{MeV}$, $m_\sigma = 600\,\mathrm{MeV}$
- $\Lambda = 500\,\mathrm{MeV}$

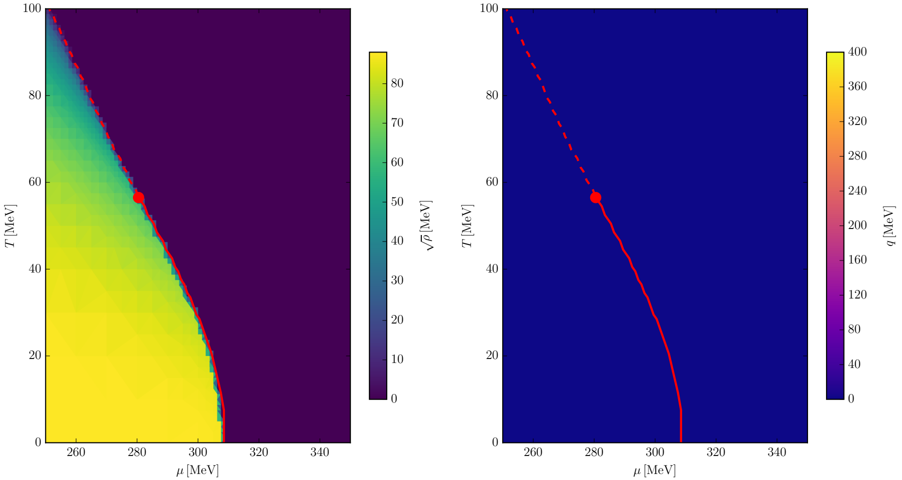

Inhomogeneous eMFA phase diagrams

- $f_\pi = 88\,\mathrm{MeV},\ M = 300\,\mathrm{MeV},\ m_\sigma = 600\,\mathrm{MeV}$
- $\Lambda = 450\,\mathrm{MeV}$

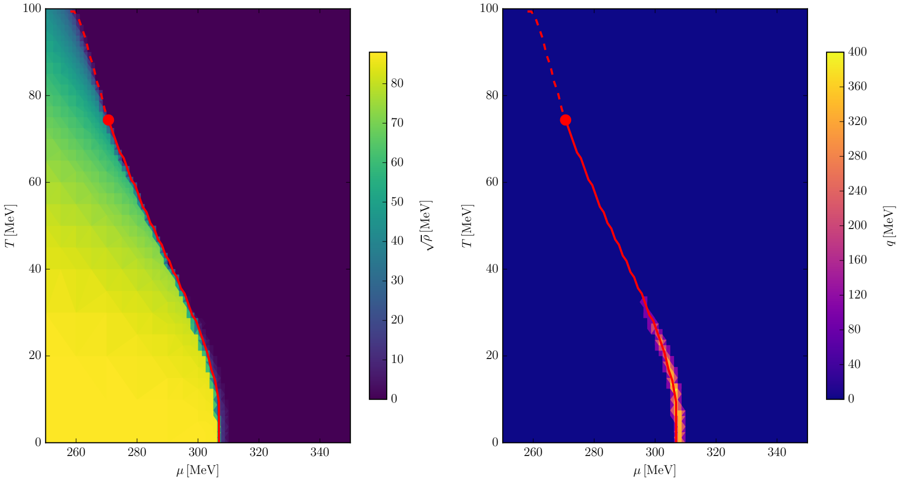

Inhomogeneous eMFA phase diagrams

- $f_\pi = 88\,\mathrm{MeV},\ M = 300\,\mathrm{MeV},\ m_\sigma = 600\,\mathrm{MeV}$
- $\Lambda = 400\,\mathrm{MeV}$

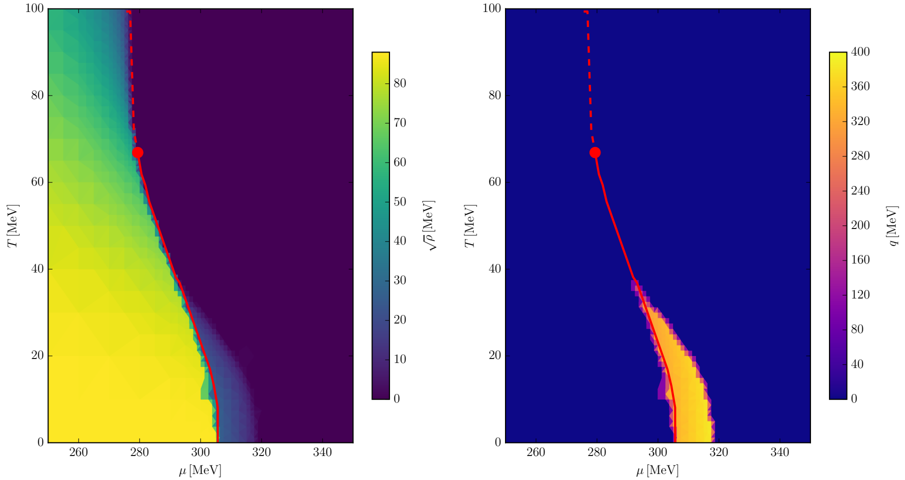

Comparison to existing eMFA results I

- eMFA with dimensional regularization using the on-shell (OS) renormalization scheme ($f_\pi = 93\,\mathrm{MeV}$, $M = 300\,\mathrm{MeV}$, $m_\sigma = 2M$)

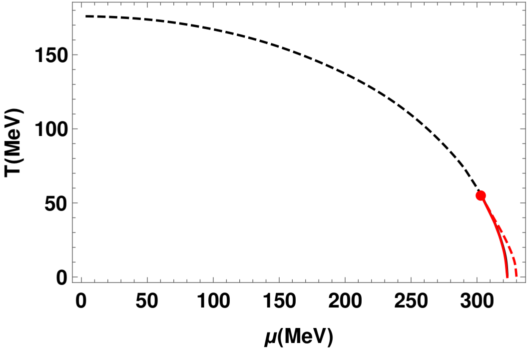

[P. Adhikari, J. O. Andersen and P. Kneschke, Phys. Rev. D (2017), arXiv: 1702.01324v2]

- Fermionic fluctuations alone should not destabilize the inhomogeneous window completely in the chiral limit

Comparison to existing eMFA results II

- eMFA with *Pauli-Villars* (PV) regularization of the vacuum term with $\Lambda_{PV} = 200\,\mathrm{MeV}$ ($f_\pi = 88\,\mathrm{MeV}$, $M = 300\,\mathrm{MeV}$, $m_\sigma = 2M$)

'RP': $f_\pi = \langle\sigma\rangle / \sqrt{Z_\pi}$ **and** $m_\sigma = m_{\sigma,\mathbf{pole}}$

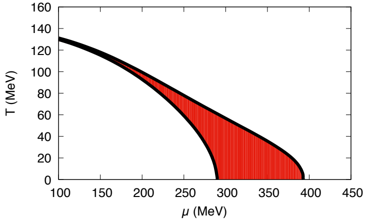

'BC': $f_\pi = \langle\sigma\rangle$ **and** $m_\sigma = m_{\sigma,\mathbf{curv}}$

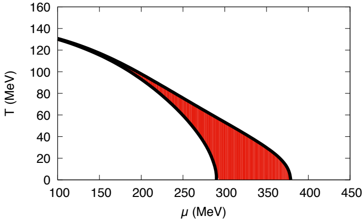

[S. Carignano, M. Buballa and W. Elkamhawy, Phys. Rev. D (2016), arXiv: 1606.08859]

- In LPA we are forced to use 'BC' parameter fitting.
- Comparison with OS/PV MF results suggests that LPA' truncation including Z_k and g_k should make a significant qualitative difference

Comparison to existing eMFA results II

- eMFA with *Pauli-Villars* (PV) regularization of the vacuum term with $\Lambda_{PV} = 300\,\mathrm{MeV}$ ($f_\pi = 88\,\mathrm{MeV}$, $M = 300\,\mathrm{MeV}$, $m_\sigma = 2M$)

'RP': $f_\pi = \langle\sigma\rangle / \sqrt{Z_\pi}$ **and** $m_\sigma = m_{\sigma,\mathbf{pole}}$

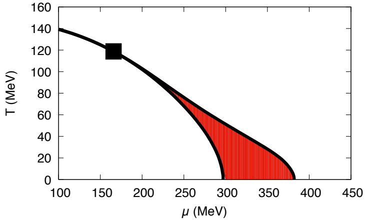

'BC': $f_\pi = \langle\sigma\rangle$ **and** $m_\sigma = m_{\sigma,\mathbf{curv}}$

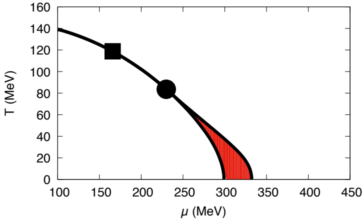

[S. Carignano, M. Buballa and W. Elkamhawy, Phys. Rev. D (2016), arXiv: 1606.08859]

- In LPA we are forced to use 'BC' parameter fitting.
- Comparison with OS/PV MF results suggests that LPA' truncation including Z_k and g_k should make a significant qualitative difference

Comparison to existing eMFA results II

- eMFA with *Pauli-Villars* (PV) regularization of the vacuum term with $\Lambda_{PV} = 400\,\mathrm{MeV}$ ($f_\pi = 88\,\mathrm{MeV}$, $M = 300\,\mathrm{MeV}$, $m_\sigma = 2M$)

'RP': $f_\pi = \langle\sigma\rangle / \sqrt{Z_\pi}$ **and** $m_\sigma = m_{\sigma,\mathbf{pole}}$

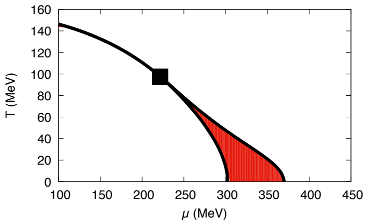

'BC': $f_\pi = \langle\sigma\rangle$ **and** $m_\sigma = m_{\sigma,\mathbf{curv}}$

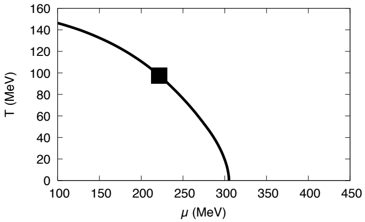

[S. Carignano, M. Buballa and W. Elkamhawy, Phys. Rev. D (2016), arXiv: 1606.08859]

- In LPA we are forced to use 'BC' parameter fitting.
- Comparison with OS/PV MF results suggests that LPA' truncation including Z_k and g_k should make a significant qualitative difference

Comparison to existing eMFA results II

- eMFA with *Pauli-Villars* (PV) regularization of the vacuum term with $\Lambda_{PV} = 5000\,\mathrm{MeV}$ ($f_\pi = 88\,\mathrm{MeV}$, $M = 300\,\mathrm{MeV}$, $m_\sigma = 2M$)

'RP': $f_\pi = \langle\sigma\rangle / \sqrt{Z_\pi}$ **and** $m_\sigma = m_{\sigma,\mathbf{pole}}$

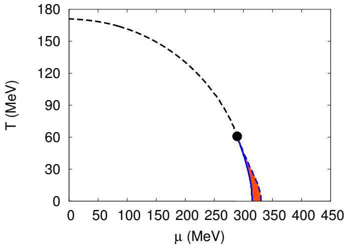

[S. Carignano, M. Buballa and W. Elkamhawy, Phys. Rev. D (2016), arXiv: 1606.08859]

- In LPA we are forced to use 'BC' parameter fitting.
- Comparison with OS/PV MF results suggests that LPA' truncation including Z_k and g_k should make a significant qualitative difference

Summary and outlook

- **What we have done so far:**
  - Derivation of a LPA flow eq. for inhomogeneous CDW condensates
  - Numerical results and parameter fixation in e/sMFA
  - First eMFA results: fermionic fluctuation in the current LPA truncation/parameter fitting scheme completely destabilize the inhomogeneous phase

- **What we plan to do next:**
  - Finish the eMFA analysis
  - Study the effects of bosonic fluctuations using the already derived LPA flow eq. for the CDW
  - Study the effects of different 3D (and 4D) regulators on the inhomogeneous phase
  - **Extending the truncation**: from LPA to LPA' (inclusion of wave-function renormalizations Z_k and running Yukawa coupling g_k)

Cubature: `github.com/stevengj/cubature`

- C package for adaptive multidimensional integration (cubature) of vector-valued integrands over hypercubes

$$\int_{a_1}^{b_1} \int_{a_2}^{b_2} \dots \int_{a_n}^{b_n} \vec{f}(\vec{x}) \, \mathrm{d}^n x$$

- Free software under the terms of the GNU General Public License (v2 or later)
- **h-adaptive integration:** recursive partitioning the integration domain into smaller subdomains, applying the same integration rule to each, until convergence is achieved
  - [A. C. Genz and A. A. Malik, J. Comput. Appl. Math. (1980)]
  - [J. Berntsen, T. O. Espelid and A. Genz, ACM Trans. Math. Soft (1991)]

Spectral decomposition of $\bar{\Omega}_{\mu,T}(\sqrt{\rho}, q)$

CRC-TR 211

$$\bar{\Omega}_{\mu,T}(\sqrt{\rho}, q) = \sum_{n_1 n_2} a^{\mu,T}_{n_1 n_2} \mathrm{T}_{2n_1}(\sqrt{\rho}) \mathrm{T}_{2n_2}(q)$$

- Decomposition using a tensor product of even-parity Chebyshev polynomials $\mathrm{T}_{2n_1}(\sqrt{\rho})$ and $\mathrm{T}_{2n_2}(q)$
- Constructed on a finite set of nodes $\{\sqrt{\rho}_{n_1}\}$ and $\{q_{n_2}\}$: *Chebychev-Gaus-Lobatto* (positive extrema) grid in ρ and q direction
- Analytic construction of $a^{\mu,T}_{n_1 n_2}$ from $\bar{\Omega}_{\mu,T}(\sqrt{\rho}_{n_1}, q_{n_2})$
- Fast computation of the function values and derivatives using the *Clenshaw algorithm*
- $\{\sqrt{\rho}_{n_1}\}$-grid will be necessary when solving the flow eq. with the bosonic loop

Spectral decomposition of $\bar{\Omega}_{\mu,T}(\sqrt{\rho}, q)$

- Inhomogeneous sMFA potential $f_\pi = 88\,\mathrm{MeV}$, $M = 300\,\mathrm{MeV}$ and $m_\sigma = 700\,\mathrm{MeV}$ at $\mu = 311\,\mathrm{MeV}$ and $T = 0\,\mathrm{MeV}$
- Chebyshev interpolation of $\bar{\Omega}^{\mathrm{sMFA}}_{311,0}(\sqrt{\rho}, q)$ with 32×16 nodes:

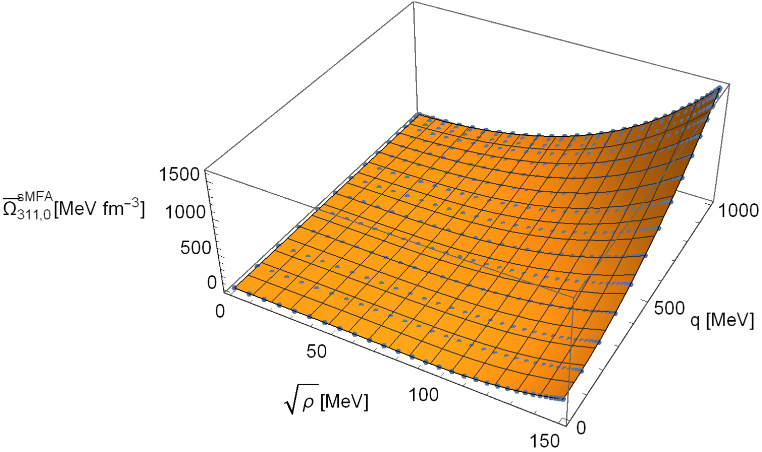

Spectral decomposition of $\bar{\Omega}_{\mu,T}(\sqrt{\rho}, q)$

CRC-TR 211

- Inhomogeneous sMFA potential $f_\pi = 88\,\mathrm{MeV}$, $M = 300\,\mathrm{MeV}$ and $m_\sigma = 700\,\mathrm{MeV}$ at $\mu = 311\,\mathrm{MeV}$ and $T = 0\,\mathrm{MeV}$
- Chebyshev interpolation of $\bar{\Omega}^{\mathrm{sMFA}}_{311,0}(\sqrt{\rho}, q)$ with 32×16 nodes:

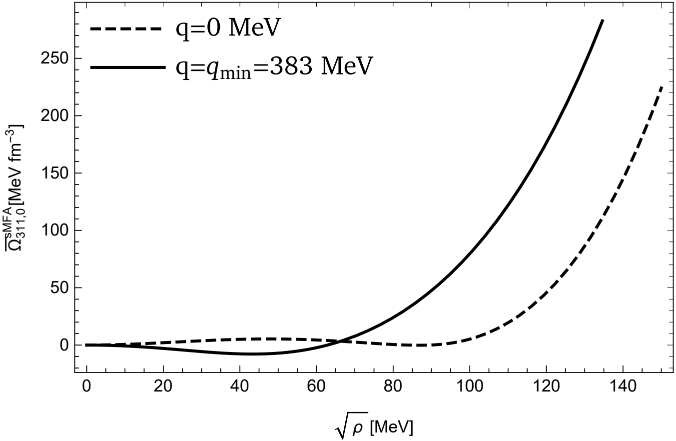

Spectral decomposition of $\bar{\Omega}_{\mu,T}(\sqrt{\rho}, q)$

- Inhomogeneous sMFA phase diagram $f_\pi = 88\,\mathrm{MeV}$, $M = 300\,\mathrm{MeV}$ and $m_\sigma = 700\,\mathrm{MeV}$

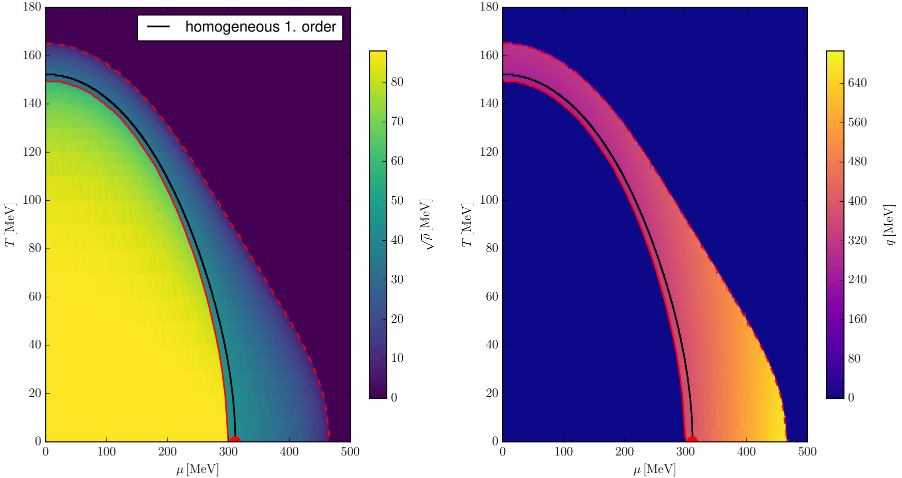

Block-Structured Adaptive Sampling

- Homogeneous sMFA phase diagram $f_\pi = 88\,\mathrm{MeV}$, $M = 300\,\mathrm{MeV}$ and $m_\sigma = 600\,\mathrm{MeV}$
- 684 points, max resolution $10 \times 10\,\mathrm{MeV}^2$, saving factor 1.0 (inital mesh)

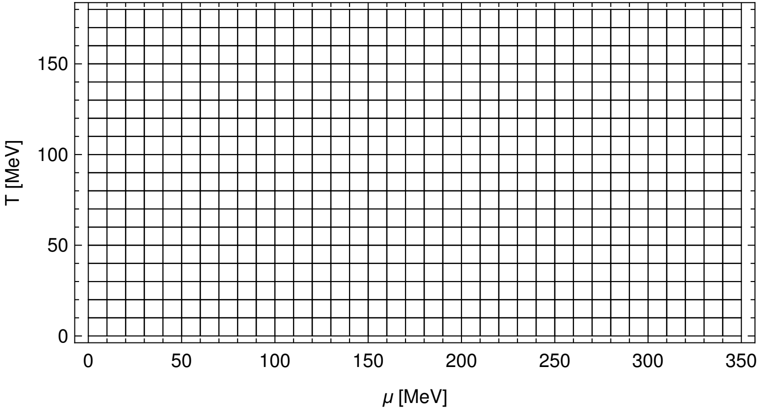

Block-Structured Adaptive Sampling

- Homogeneous sMFA phase diagram $f_\pi = 88\,\mathrm{MeV}$, $M = 300\,\mathrm{MeV}$ and $m_\sigma = 600\,\mathrm{MeV}$
- 925 points, max resolution $5 \times 5\,\mathrm{MeV}^2$, saving factor 2.8

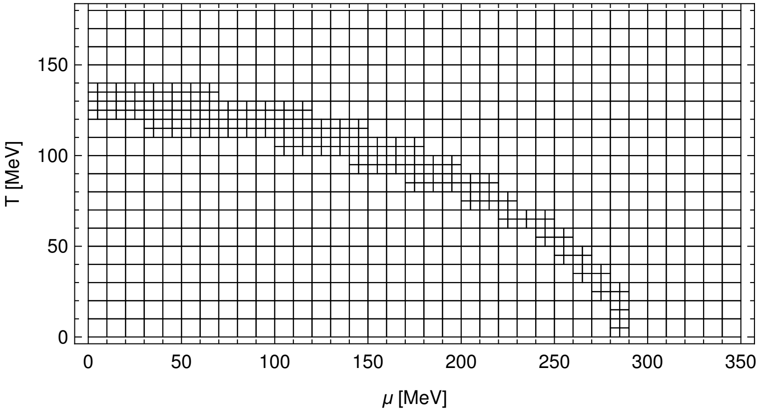

Block-Structured Adaptive Sampling

- Homogeneous sMFA phase diagram $f_\pi = 88\,\mathrm{MeV}$, $M = 300\,\mathrm{MeV}$ and $m_\sigma = 600\,\mathrm{MeV}$
- 1419 points, max resolution $2.5 \times 2.5\,\mathrm{MeV}^2$, saving factor 7.6

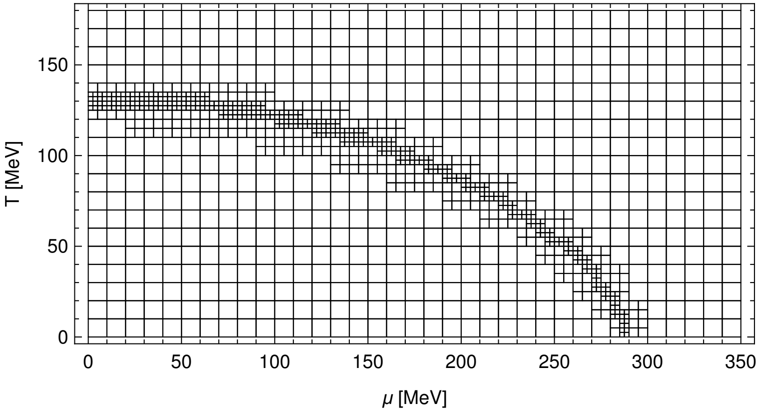

Block-Structured Adaptive Sampling

- Homogeneous sMFA phase diagram $f_\pi = 88\,\mathrm{MeV}$, $M = 300\,\mathrm{MeV}$ and $m_\sigma = 600\,\mathrm{MeV}$
- 2278 points, max resolution $1.25 \times 1.25\,\mathrm{MeV}^2$, saving factor 17.9

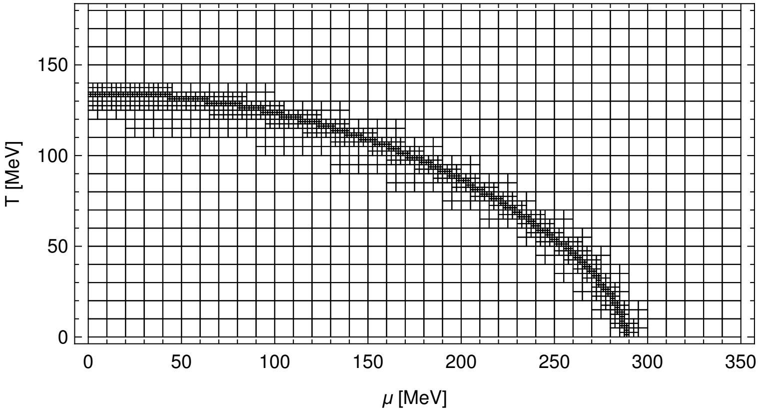

Block-Structured Adaptive Sampling

- Homogeneous sMFA phase diagram $f_\pi = 88\,\mathrm{MeV}$, $M = 300\,\mathrm{MeV}$ and $m_\sigma = 600\,\mathrm{MeV}$
- 2278 points, max resolution $1.25 \times 1.25\,\mathrm{MeV}^2$, saving factor 17.9

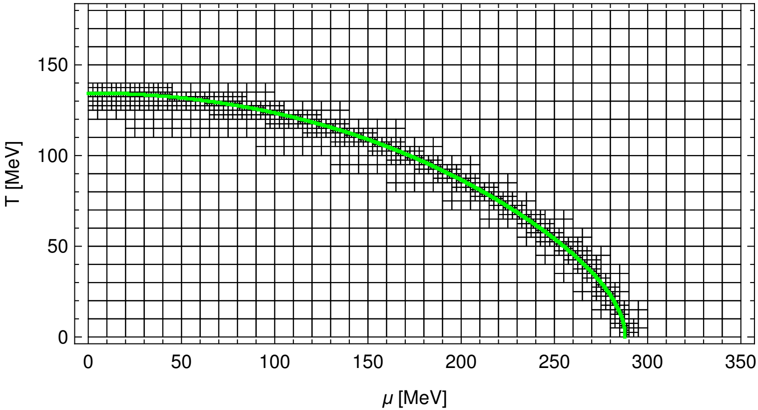

Homogeneous eMFA phase diagram at very low Λ

- $f_\pi = 88\,\mathrm{MeV}$, $M = 300\,\mathrm{MeV}$, $m_\sigma = 600\,\mathrm{MeV}$ and $\Lambda = 200\,\mathrm{MeV}$